LAWRENCE
LIVERMORE
NATIONAL
LABORATORY

UCRL-CONF-201585

Flame Inhibition by Phosphorus-Containing Compounds in Lean and Rich Propane Flames

O.P. Korobeinichev, V.M. Shvartsberg, A.G. Shmakov, T.A. Bolshova, T.M. Jayaweera, C.F. Melius, W.J. Pitz, C.K. Westbrook, H. Curran

December 22, 2003

30th International Symposium on Combustion
Chicago, IL, United States
July 25, 2004 through July 30, 2003

Flame Inhibition by Phosphorus-Containing Compounds in Lean and Rich Propane Flames

O.P. Korobeinichev, V. M. Shvartsberg, A.G. Shmakov, T.A. Bolshova

Institute of Chemical Kinetics & Combustion
Novosibirsk, 630090 Russia

T.M. Jayaweera, C. F. Melius, W.J. Pitz, C.K. Westbrook*

Lawrence Livermore National Laboratory
PO Box 808, Livermore, CA 94551-0808 USA

H. Curran

Department of Chemistry
National University of Ireland, Galway
Galway, Ireland.

Colloquium: Fire Research

Short Running Title: Flame Inhibition by Phosphorus Compounds

Total Word Count:

Text:	MS word count	3853
Equations:	(13 + 8 blank lines) x 7.6	160
References:	(40+2) x 2.3 x 7.6	734
Figures:	1: 6.1" wide x 5.0" high + 20 word caption	156
	2: 6.3" wide x 5.0" high + 20 word caption	152
	3: 6.3" wide x 4.7" high + 20 word caption	145
	4: 4.8" wide x 4.0" high + 20 word caption	158
	5: 6.0" wide x 4.2" high + 17 word caption	136
	6: 6.2" wide x 5.0" high + 26 word caption	160
	7: 6.2" wide x 5.0" high + 26 word caption	160
Table:	65 mm column length at 67 mm width	145

Total word count: 5959 words

*corresponding author
Tel: 925-422-4108
Fax: 925-422-2644
Email: westbrook1@llnl.gov

ABSTRACT

Chemical inhibition of laminar propane flames by organophosphorus compounds has been studied experimentally, using a laboratory Mache Hebra nozzle burner and a flat flame burner with molecular beam mass spectrometry (MBMS), and with a computational flame model using a detailed chemical kinetic reaction mechanism. Both fuel-lean and fuel-rich propane flames were studied to examine the role of equivalence ratio in flame inhibition. The experiments examined a wide variety of organophosphorus compounds. We report on the experimental species flame profiles for tri-methyl phosphate (TMP) and compare them with the species flame profile results from modeling of TMP and di-methyl methyl phosphonate (DMMP). Both the experiments and kinetic modeling support and illustrate previous experimental studies in both premixed and non-premixed flames that inhibition efficiency is effectively the same for all of the organophosphorus compounds examined, independent of the molecular structure of the initial inhibitor molecule. The chemical inhibition is due to reactions involving the small P-bearing species $HOPO_2$ and HOPO that are produced by the organophosphorus compounds (OPCs). The ratios of the $HOPO_2$ and HOPO concentrations differ between the lean and rich flames, with $HOPO_2$ dominant in lean flames while HOPO dominates in rich flames. The resulting $HOPO_2$ and HOPO species profiles do not depend significantly on the initial source of the $HOPO_2$ and HOPO and thus are relatively insensitive to the initial OPC inhibitor. A more generalized form of the original Twarowski mechanism for hydrocarbon radical recombination is developed to account for the results observed, and new theoretical values have been determined for heats of formation of the important P-containing species, using the BAC-G2 method.

Keywords: Phosphorus, inhibition, premixed flames, thermochemistry, modeling

Introduction

For many years, halogenated hydrocarbons, especially CF_3Br, were used as the preferred means of fire suppression, until their role in atmospheric ozone depletion ended their manufacture with the 1990 Montreal Protocol. The search for effective replacements has led to a family of organophosphorus compounds (OPCs) which have shown considerable promise as flame inhibitors [1]. Early work of Twarowski [2-4] showed that phosphine (PH_3) accelerated radical recombination in hydrogen oxidation, and subsequent work by Korobeinichev et al. began to explain how OPCs inhibited hydrogen flames [5,6] and hydrocarbon flames [7].

Chemically active flame inhibitors alter flame chemistry by catalytic recombination of key flame radicals, especially H and O atoms and OH radicals. H atoms are particularly important in flame propagation, since the principal chain branching reaction in hydrogen and hydrocarbon flames is $H + O_2 \rightarrow OH + O$. Fast elementary reactions interconnect these small radical species, and removal of any of them through recombination reduces concentrations of all of them correspondingly. Therefore, radical recombination leads to fewer H atoms in the reaction zone, which leads to reduced chain branching and a lower burning velocity. This applies to familiar halogenated suppressants such as HBr and CF_3Br [8,9], sulfur compounds such as SO_2 [10,11], and OPCs such as dimethyl methylphosphonate (DMMP) and trimethyl phosphate (TMP).

Twarowski [2-4] established that catalytic recombination of radicals by phosphine (PH_3) is accomplished by reactions of small P-containing species produced from the additive, particularly

$$H + PO_2 + M \rightarrow HOPO + M \quad (1a)$$

$$HOPO + H \rightarrow H_2 + PO_2 \quad (1b)$$

$$OH + PO_2 \ (+ M) \rightarrow HOPO_2 \ (+ M) \quad (2a)$$

$$H + HOPO_2 \rightarrow H_2O + PO_2 \quad (2b)$$

which consume highly reactive H atoms and OH radicals to produce stable H_2 and H_2O. In most kinetic modeling studies of inhibition by OPC additives, an additional reaction between HOPO and OH to produce PO_2 and water is also included. The same small species act in the same general way with the introduction of other parent OPCs such as TMP, DMMP, and in chemical warfare agents such as sarin [12], as a considerable number of recent studies have reported [13-26].

Most investigations of flame inhibition by OPCs have been carried out in flames under stoichiometric conditions or in static or flow reactors in which diffusional transport is not important. The present study examines the effect of fuel/oxygen ratios on the chemical kinetics of inhibition by OPCs in laminar flames and how that suppression may change for different equivalence ratios and different OPCs. In lean hydrocarbon flames, OH radicals and O atoms normally dominate the reacting radical pool while H atoms are most prevalent in rich conditions.

Thus, it is possible that different reaction cycles may be responsible for flame inhibition at different equivalence ratios.

We therefore have investigated the flame inhibition kinetic pathways for both rich and lean propane flames, using TMP and DMMP as flame inhibitors. A key aspect of this work is the identification of the P-containing species (PO_XH_Y) involved in the proposed reaction pathways (e.g., reactions 1 and 2 above). Past kinetic studies of flame inhibition by OPCs have been limited by lack of reliable experimental data for PO_XH_Y species concentrations. For example, Noguiera and Fisher [18] compared measured hydrocarbon species profiles from a DMMP-doped CH_4/air, burner-stabilized, premixed flame to numerical model predictions. Significant differences between the experimental and numerical results were observed, but the errors could not be reduced since the P-containing species concentrations could not be measured.

The present work reports results from experimental studies of premixed laminar propane flames carried out in the Novosibirsk laboratory of O. Korobeinichev. Spatial profiles of major species concentrations were measured, including many of the important OPCs in the flames. The equivalence ratios represent both fuel-lean and fuel-rich mixtures. A wide variety of OPC inhibitors were employed. We focus on the experimental results for undoped propane flames and the same flames doped with TMP. An existing chemical kinetic model was updated, including new PO_XH_Y thermochemistry, to describe the experimental results and provide insights into OPC-doped flame inhibition.

Experiments

Premixed laminar flames were stabilized on a flat Botha-Spolding flat-flame burner 16 mm in diameter at atmospheric pressure and slightly elevated unburned gas temperatures of about 380K. Combustible C_3H_8/O_2/Ar mixtures (lean, 0.025/0.136/0.839, $\phi \sim 0.9$, and rich, 0.029/0.121/0.85, $\phi \sim 1.2$) were prepared using mass flow controllers, with a total volumetric flow rate of 1.5 slpm. TMP (1200 ppm) was added to the combustible mixtures using a saturator with liquid TMP in a controlled temperature bath. Temperature profiles in the flames were measured by Pt-Pt+10%Rh thermocouples welded from wire 0.02 mm in diameter, covered by a thin layer of SiO_2 to prevent catalytic recombination of radicals on their surfaces. The resulting thermocouple junction has a diameter of 0.03 mm and a shoulder length of about 3 mm, providing negligible heat losses to the cold contacts. Further details of the thermocouple design can be found elsewhere [5].

Chemical species profiles were measured by MBMS, using soft ionization by electron impact reported previously [19]. Synchronous demodulation was applied to measure flame species in low concentration up to 10 ppm with a mean square error not more than 50%, and stable species with standard deviations not more than 10%. Quartz cones with inner angles of 40° and 45°, wall thickness of 0.05 mm and orifice diameter 0.05 – 0.09 mm were used as probes. It was found that in these atmospheric experiments, the lifetime of the quartz probe is limited by the formation of a solid film of pyrophosphoric acids, especially near the probe tip, which alloys with heated quartz to form easily melted phosphate glass. Disturbance of the flames by the probe has been taken into account [27].

In a separate set of experiments, the laminar burning velocity of premixed C_3H_8/air flames was measured using a Mache-Hebra nozzle burner [28] and the total area method from an image of the flame [29]. The experimental technique is described in detail elsewhere [21]. To evaluate the influence of heat loss from the flame to the burner on the measured values, the speed of propane-air undoped flames of various stoichiometries was measured for T_0=298 K. The obtained results of 41.7 cm/sec for a stoichiometric undoped flame agrees quite well with experimental data measured by different techniques [30-32] and the computed value described below, giving some validity to this technique for measurement of flame burning velocities.

Modeling Approach

The Chemkin Premix code [33] was used to compute the species profiles and reaction fluxes for burner-stabilized and freely propagating laminar flames. Experimentally measured temperatures were used as input for the burner-stabilized flames. A recently refined high temperature propane oxidation mechanism [34] was used for the hydrocarbon species, with updated thermodynamics parameters. At T=300 K, P=1 atm, this mechanism computes a laminar burning velocity of 41.1 cm/sec, in good agreement with our own experimental values above and other experimental studies. Further validation has been performed comparing the mechanism with shock-tube studies [34].

Improvements in thermochemistry for the phosphorus compounds were made, using the BAC-G2 method [35]. Results for enthalpies of formation of the small phosphorus species are summarized in Table 1. Included in the table are values found previously using other quantum chemical methods, including BAC-MP4 by Melius [36], G3X by Mackie et al. [37] and CBS by Bauschlicher [38].

Our kinetic reaction mechanism is based on previous models [12,13,17,22,23] for combustion inhibition with OPCs. The hydrocarbon reactions for each model differ slightly in each case, and the reactions by which the initial OPC consumption occurs also differ slightly, but all are based on the core reaction cycles identified originally by Twarowski.

The major change we have made is to refine the reaction kinetic pathway by which $HOPO_2$ can be converted to PO_2 and H_2O, clarifying the meaning of reaction 2b above. Like many other apparently simple reactions, the overall reaction of H with $HOPO_2$ actually proceeds by a rather complex process that begins by adding the H atom to the $HOPO_2$ species, forming an adduct in a metastable, excited energy state. From the point of view of theoretical chemical kinetics, the reaction then proceeds on a potential energy surface with multiple local potential energy "wells", or local minima. Each such minimum defines a distinct metastable arrangement of the species of the adduct formed by the reactants. A metastable species can be collisionally stabilized, it can continue to rearrange itself in a number of possible ways, and it can complete the overall reaction by breaking into final, relatively stable products. In the case of the reaction of H with $HOPO_2$, the H atom can add directly to the phosphorus atom in $HOPO_2$ to form HPO(OH)O, which can then undergo a 1,2-hydrogen shift to form $PO(OH)_2$, and then a four-centered water elimination step to produce H_2O and PO_2. The initial addition step has no activation energy barrier, while the hydrogen shift and water elimination have barrier heights of about 1 kcal/mol above the reactants' energy. This sequence of steps can be represented by the reaction sequence

$$HOPO_2 + H \leftrightarrow HPO(OH)O \leftrightarrow PO(OH)_2 \rightarrow H_2O + PO_2 \qquad (2b')$$

in which some of the steps are reversible because they represent further rearrangements on the potential energy surface. As part of the present study, we have calculated the highest energy barrier between reactants and products of reaction 2b' to be less than 2 kcal/mol. To our knowledge, it has not previously been proposed as a viable reaction pathway for this reaction, and since it has little or no activation barrier, it was found to be an important contributor to the flame inhibition kinetics.

A different initial reaction step, in which the H atom adds directly to one of the O atoms in $HOPO_2$, results in $PO(OH)_2$, followed by the same four-center water elimination step to produce H_2O and PO_2. This sequence can be represented in the form

$$HOPO_2 + H \leftrightarrow PO(OH)_2 \rightarrow H_2O + PO_2 \qquad (2b'')$$

The energy barrier to this reaction pathway has recently been computed by Mackie et al. [37] to be approximately 12.2 kcal/mol.

If reactions 2b' and 2b" were irreversible and went directly to their products $H_2O + PO_2$, then both could be written as single-step reactions, avoiding the complexity of writing the multiple steps. The highest energy barrier in each sequence of steps would be the overall activation energy, and the A-factor could then be determined either by comparison with experiments or additional chemical theory. Twarowski and other early modeling studies reached an equivalent approach by assuming from the begininning that this was an elementary reaction. Twarowski assumed a rate expression of 2 x 1013 exp(-50 kJ/mol/RT) and found rates of radical consumption that agreed quite well with observations. The 50 kJ/mol is equal to approximately

12 kcal/mol, remarkably close to the value derived theoretically by Mackie et al. Twarowski's value for this reaction rate was then used until the present, with minor modifications, although Korobeinichev et al. [20] carried out some preliminary computations with a considerably lower A-factor for this reaction, and then later [22] restored it to a value close to its present value in the present model.

The present study has used a related approach in its implementation of the reaction of H with $HOPO_2$. We have included reaction 2b' as a single step reaction producing $H_2O + PO_2$ but using an energy barrier of zero to reflect the energetics of the reaction path leading through the HPO(OH)O intermediate. We have also included reaction 2b", but we have implemented it in two steps, the first producing $PO(OH)_2$ and the second step continuing to $H_2O + PO_2$. We have done this because it appears that the intermediate species $PO(OH)_2$ can react with radical species on times scales comparable with its 4-center water elimination reaction. The reaction rate of the first step of our reaction 2b" is very similar to that originally proposed by Twarowski, but with an activation energy of 9 kcal/mol which was a result of our BAC-G2 thermochemical calculations.

In a particularly elegant recent theoretical study, Mackie et al. [37] first introduced the concept of reaction 2b proceeding through an intermediate activated complex and identified that complex as $PO(OH)_2$. Their goal was to identify possible reaction pathways for small P-containing species that were more rapid than the simplified overall reaction steps. Our rate expression for the reaction path identified by Mackie et al. agrees quite well with their calculations. Our identification of another, even lower energy barrier pathway has provided

another fast route for the second half of the catalytic inhibition cycle 2 and contributed significantly to the computed results in the present study.

We must point out that it now appears that none of the other 3 reactions identified by Twarowski, reactions 1a, 1b and 2a, are likely to proceed as elementary reactions and will require considerable further theoretical study. Recently, Haworth et al. [39] presented theoretical analyses of these reactions with predictions of their reaction rates under flame conditions, which will be very helpful in future modeling analyses of these systems.

We also added reactions involving the diphosphorus oxide compounds P_2O_3, P_2O_4 and P_2O_5, which have relatively strong bond-dissociation energies of 77, 74 and 92 kcal/mol, respectively (see Table I), to see if they play a role in the overall chemical kinetics. The entire hydrocarbon and OPC reactions mechanism can be obtained electronically from the authors.

Results and Discussion

The new kinetic model, with updated thermochemistry, was used to calculate the structures of the lean and rich propane flames, with and without 1200 ppm TMP in the unburned gases. For all of the flames, the computed results for the major reactant and product species and the spatial extent of each flame were in excellent agreement with the experimentally observed values, as shown in Figures 1 and 2.

Computed species mole fractions are shown together with the experimental values of the P-bearing species for the lean and rich inhibited flames in Figures 3 and 4. Overall agreement between experimental and computed values is very good for all of the species in the lean flame. However, there are significant disparities between the model results and experimental data in the

rich flame. To ensure that all possible P-bearing species were included, we included the P_2O_3, P_2O_4 and P_2O_5 species within the model. We found that their concentrations were insignificant (several orders of magnitude smaller than the PO, PO_2 and PO_3 species), in both the lean and rich flames. Thus the diphosphorus species cannot account for the discrepancies in the rich flame. The low concentrations of the diphosphorus species is due to the high product temperatures and the low partial pressures of the phosphorus oxides. At higher dopant concentrations and flame pressures, the diphosphorus species could become important.

We find in the model that the POxHy species reach their thermochemical equilibrium values at large distances from the burner. The good agreement between theory and experiment in the lean flame (Fig. 3) appears to validate the new thermochemistry for the POxHy species predicted by the BAC-G2 method (Table I). However, the agreement for the rich flame (Fig. 4) is not very good. At large distances from the burner, we expect the POxHy species ratios to be at their thermodynamic equilibrium, not depending on the reaction mechanism. Given this good agreement for the lean flame, we believe the modeled ratios of the POxHy species to be more reasonable, since the model uses the same thermochemistry for both flames. On the other hand, the modeling results for the POxHy species profiles in the region near the reaction zone are quite sensitive to slight modifications in the reaction mechanism. Thus the shapes of the computed profiles near the reaction zone could be incorrect. Further studies, both of the experimental profile measurements and of the computational reaction mechanism, must be carried out to determine the casue of the discrepancy.

To further understand the nature of the P-bearing species with respect to the inhibition mechanism, we also considered other OPCs. A recent study [40] showed that many different

organophosphate compounds are approximately equal in inhibition effectiveness for hydrocarbon flames. This is illustrated in Figure 5, which shows the relative reductions in burning velocity from addition of other inhibitors to a stoichiometric propane/air mixture. Burning velocity reductions produced by other OPC additives, many of them including F atoms in addition to P atoms (one of them is shown in Fig. 5) were very similar to the purely OPC results shown here. These results are compared to the reduction in burning velocity produced by addition of CF_3Br, which is clearly much less effective than any of the OPC additives, and the inhibition produced by addition of iron pentacarbonyl, which is much more effective.

To investigate the reasons for the inhibition similarities of the different OPCs, we modeled the same propane/O_2/Ar flames but used DMMP as the dopant rather than TMP. The resulting P-bearing species profiles in the DMMP-doped flames are compared with those from the TMP-doped flames in Figures 6 and 7 for the lean and rich flames. The similarities in the P-bearing species mole fractions in these flames are striking. In both the lean and rich pairs of flames, both additives are consumed at exactly the same rates, and the levels of PO2, HOPO and $HOPO_2$ are also effectively equal in the two flames and eventually reach exactly the same equilibrium levels in the burned gases.

These similarities are perhaps unexpected, since TMP decomposes primarily to produce $HOPO_2$, while HOPO is the primary product of DMMP (see Figs. 5 and 6 of [12]). Yet in spite of the differences in the initial decomposition products of the OPCs, both inhibited lean flames show the predominant formation of $HOPO_2$, while the rich flames show the predominant formation of HOPO. The slight differences in Figs. 6 and 7 between TMP- and DMMP-

inhibited flames represent the residual effects of the different decomposition products of the inhibitor. These differences disappear quickly as the catalytic recombination reaction cycles rapidly equilibrate the relative levels of PO_2, HOPO and $HOPO_2$. The relative levels of these OPCs in the products is determined by their equilibrium constants and the overall equivalence ratio in the flame, not by the structure or composition of the OPC additive.

These computations demonstrate clearly that the flame inhibition kinetics for both additives depend on the reactions and thermochemistry of HOPO, $HOPO_2$, PO_2 and other small species, and not on the details of the molecular structure of the initial organophosphorus compound. The core inhibition mechanism for all of these compounds in Fig. 5 is the same set of catalytic recombination cycles of reactions, and the only major distinction between different organophosphate inhibitors appears to depend on how rapidly these catalytic cycles are established in a given flame. The different inhibitors in Fig. 5 have different hydrocarbon contents, and this will have a minor influence on their inhibition efficiencies because their different C/H/O compositions can affect the equilibrium between HOPO and $HOPO_2$, and additional components such as F atoms will also have minor influences on inhibition efficiencies. However, as shown in Fig. 5 and illustrated in Figs. 6 and 7, the primary inhibition mechanisms for all of these organophosphorus compounds are exactly the same. As noted above, the flames with TMP additive initially generate $HOPO_2$, while DMMP initially produces HOPO, yet both inhibit the propane flames nearly identically because of the very rapid interconversion of the small P-containing species.

The coupling between HOPO and $HOPO_2$ is dominated by the same reactions that are responsible for the flame inhibition. The basic inhibitor reactions catalytically convert $HOPO_2$ and HOPO into PO_2 via the consumption of H, OH and O and then back to $HOPO_2$ and HOPO via the consumption of OH and H. The net reactions in each case are the conversion of radicals H, OH and O into H_2O and H_2, thereby reducing the radical pool available to propagate the flame. The dominant cycles of inhibition can still be represented by reactions 1 and 2 but they should be viewed as global reactions involving multiple pathways, with chemically activated intermediates such as $PO(OH)_2$ and HPO(OH)O that may be collisionally stabilized during individual trips through the cycles. Since both cycles share the same PO_2 intermediate catalytic species, it is not at all surprising that $HOPO_2$ and HOPO are quickly interconverted as shown in Figs. 6 and 7. The resulting inhibition mechanism can be summarized by a generalization of the original Twarowski model:

$$H + PO_2 + M \rightarrow HOPO + M \qquad (1a)$$

$$HOPO + H \rightarrow H_2 + PO_2 \qquad (1b)$$

$$HOPO + OH \rightarrow H_2O + PO_2 \qquad (1c)$$

$$OH + PO_2 + M \rightarrow HOPO_2 + M \qquad (2a)$$

$$HOPO_2 + H \rightarrow H_2O + PO_2 \qquad (2b)$$

$$HOPO_2 + H \leftrightarrow HPO(OH)O \leftrightarrow PO(OH)_2 \rightarrow H_2O + PO_2 \qquad (2b')$$

$$HOPO_2 + H \leftrightarrow PO(OH)_2 \rightarrow H_2O + PO_2 \qquad (2b'')$$

It should also be noted that we have discussed the complexity of reaction 2 where the second half of that inhibition cycle takes place on a complicated potential energy surface. However, the same situation applies to the other reactions 1a, 1b and 2a of the Twarowski reactions above. In fact, in addition to a direct abstraction reaction, reaction 1c can take place on the same potential energy surface as the second half of cycle 2, with the same overall products but with a different input channel. We have also given most attention to the catalytic recombination reaction cycles that produce water, but if H is replaced by other hydrocarbon radicals in these recombination cycles, radical recombination can form methane, methanol and other stable species, which will also result in flame inhibition. For example, when HBr is replaced by CH_3Br as an additive, flame inhibition reactions produce a net recombination reaction of $CH_3 + H = CH_4$, and the same should be expected for OPC-catalyzed inhibition as well. Further experimental and kinetic modeling work is needed to understand the intricacies of these reactions.

Conclusions

A study of flame inhibition in propane flames by organophosphorus compounds has been carried out experimentally and numerically, with particular attention to variations in inhibition between rich and lean conditions. Numerically, the mechanism by which the OPC acts under different equivalence ratios was explored. Species profiles for the POxHy species, as well as the OPC dopant were measured for TMP in both rich and lean propane flames. Comparisons of the species profiles with numerical models gave excellent agreement for the lean flame. However, discrepancies remain for the rich flame, and further work to resolve these discrepancies has been

proposed. Overall, though, both the experiment and the modeling showed that the TMP decomposed early in the flame, with $HOPO_2$ becoming the dominant inhititor species in the lean flame and HOPO becoming dominant in the rich flame. Flame speeds of propane flames with different OPC additives showed very similar inhibition efficiency, and computational comparisons between TMP and DMMP as inhibitors showed dramatically similar behavior. New thermochemistry for the OPCs was calculated, using the BAC-G2 method, and new reaction sequences were added, which improved agreement between experiment and calculation. Although the same key catalytic cycles are observed for equivalence ratios of both ϕ=0.9 and ϕ=1.2, there is a systematic variation in the details of the different catalytic reaction sequences involved. These details can be incorporated into a more generalized form of the inhibition reaction system originally postulated by Twarowski.

Acknowledgments

The computational portions of this work were supported by the Office of Basic Energy Sciences, Division of Chemical Sciences, and performed under the auspices of the U. S. Department of Energy by the University of California, Lawrence Livermore National Laboratory under Contract No. W-7405-Eng-48. The experimental part of this work was carried out with support from the Civilian Research and Development Foundation under grant RC1-2386-NO-02 and by US Army Research Office under grant DAAD 19-00-1-0136, Modification No. P00001. HC acknowledges support from Enterprise Ireland under their Research Scholarship and International Collaboration Programmes.

References

1. Hastie, J.W., and Bonnell, D.W., *Molecular Chemistry of Inhibited Combustion Systems*, National Bureau of Standards, NBSIR 80-2169 (1980).
2. Twarowski, A.J., *Combust. Flame* 94, 91-107 (1993).
3. Twarowski, A.J., *Combust. Flame* 94, 341-348 (1993).
4. Twarowski, A.J., *Combust. Flame* 102, 41-54 (1995).
5. Korobeinichev, O.P., Ilyin, S.B., Mokrushin, V.V., and Shmakov, A.G., *Combust. Sci. Technol.* 116, 51-61 (1996).
6. Korobeinichev, O.P., Shvartsbert, V.M., Chernov, A.A., and Mokrushin, B.B., *Proc. Combust. Inst.* 26, 1035-1042 (1996).
7. Korobeinichev, O.P., Bolshova, T.A., Shvartsberg, V.M., and Chernov, A.A., *Combust. Flame* 125, 744-751 (2001).
8. Westbrook, C. K., *Proc. Combust. Inst.* 19: 127-141 (1982).
9. Westbrook, C.K., *Combust. Sci. Technol.* 34, 201-225 (1983).
10. Smith, O.I., Wang, S.-N., Tseregounis, S., and Westbrook, C.K., Combust. Sci. Technol. 30, 241-271 (1983).
11. Glarborg, P., Kubel, D., Dam-Johansen, K., Chiang, H.-M., and Bozzelli, J.W., *Int. J. Chem. Kinet.* 28, 773-790 (1996).
12. Glaude, P.A., Melius, C., Pitz, W.J., and Westbrook, C.K., *Proc. Combust. Inst.* 29, 2469-2476 (2002).
13. Werner, J.H., and Cool, T.A., *Combust. Flame* 117, 78-98 (1999).
14. Zegers, E.J.P., and Fisher, E.M., Combust. Flame 116, 69-89 (1996).

15. MacDonald, M.A., Jayaweera, T.M., Fisher, E.M., and Gouldin, F.C., Proc. Combust. Inst. 27, 2749-2756 (1998).

16. MacDonald, , M.A., Fisher, E.M., and Gouldin, F.C., *Combust. Flame* 124, 668-683 (2001).

17. Wainner, R.T., McNesby, K.L., Daniel, A.W., Miziolek, A.W., and Babushok, V.I., *Halon Options Technical Working Conference (HOTWC)*, Albuquerque, NM, 2000, pp. 141-153.

18. Nogueira, M.F.N., and Fisher, E.M., *Combust. Flame* 132, 352-363 (2003).

19. Korobeinichev, O.P., Ilyin, S.B., Shvartsbert, V.M., and Chernov, A.A., Combust. Flame 118, 718-726 (1999).

20. Korobeinichev, O.P., Ilyin, S.B., Bolshova, T.A., Shvartsberg, V.M., and Chernov, A.A., *Combust. Flame* 121, 593-609 (2000).

21. Korobeinichev, O.P., Mamaev, A.L., Sokolov, V.V., Bolshova, T.A., and Schvartsberg, V.M., *Halon Options Technical Working Conference (HOTWC)*, Albuquerque, NM, 2001, pp. 173-186.

22. Korobeinichev, O.P., Bolshova, T.A., Shvartsberg, V.M., and Shmakov, A.G., *Halon Options Technical Working Conference (HOTWC)*, Albuquerque, NM, 2002, http://www.bfrl.nist.gov/866/HOTWC/pubs/24_Korobeinichev_et_al.pdf

23. Korobeinichev, O.P., Shvartsberg, V.M., Bolshova, T.A., Ahmakov, A.G., and Knyazkov, D.A., Combust. Expl. Shock Waves 38, 127-133 (2002).

24. Glaude, P.A., Curran, H.J., Pitz, W.J., and Westbrook, C.K., *Proc. Combust. Inst.* 28, 1749-1756 (2000).

25. MacDonald, M.A., Jayaweera, T.M., Fisher, E.M., and Gouldin, F.C., Combust. Flame 116, 166-176 (1999).

26. Jayaweera, T.M., Flame Suppression by Aqueous Solutions, Ph.D. thesis, Cornell University, Ithaca, NY, 2002.

27. Korobeinichev, O.P., Tereshenko, A.G., Emelyanov, I.D., Fedorov, S.Y., Kuibida, L.V., and Lotov, V.V., *Combust. Expl. Shock Waves* 21, 524-530 (1985).

28. Mache, H., and Hebra, A., *Sitzungsber. Osterreich. Akad. Wiss., Abt.* IIa, 150 (1941) 157.

29. Linteris, G.T., and Truett, G.T., *Combust. Flame* 105, 15-27 (1996).

30. van Maaren, A., and deGoey, L.P.H., *Combust. Sci. Technol.* 102, 309-314 (1994).

31. Vagelopoulos, C.M., and Egolfopoulos, F.N., *Proc. Combust. Inst.* 25, 1341-1347 (1994).

32. Dyakov, I.V., Konnov, A.A., de Ruyck, J., Bosschaart, K.J., Brock, E.C.M., and de Goey, L.P.H., *Combust. Sci. Technol.* 172, 81-96 (2001).

33. Kee, R.J., Rupley, F.M., Miller, J.A., Sandia National Laboratories SAND89-8009B (1989).

34. Curran, H.J., *Proceedings of the European Combustion Meeting*, 2003.

35. Melius, C., and Allendorf, M.D., *J. Phys. Chem. A* 104, 2168-2177 (2000).

36. Melius, C., in *Chemistry and Physics of Energetic Materials* (S.N. Bulusu, Ed.), Klumer Academic Publishers, Dorderech, The Netherlands, 1990, p. 21.

37. Mackie, J.C., Bacskay, G.B., and Haworth, N.L., *J. Phys. Chem. A* 106, 10825-10830(2002).

38. Bauschlicher, C.W., *J. Phys. Chem. A* 103 (50), 11126-11129 (1999).

39. N.L. Haworth, G.B. Bacskay and J.C. Mackie, *J. Phys. Chem. A* 106, 1533-1541 (2002).

40. Shmakov, A.G., Korobeinichev, O.P., Bolshova, T.A., Shvartsberg, V.M., *Halon Options Technical Working Conference (HOTWC)*, Albuquerque, NM, 2002, http://www.bfrl.nist.gov/866/HOTWC/pubs/25_Shmakov_et_al.pdf

Figure Captions

1. Spatial variations of stable species in the lean ($\phi = 0.9$) propane flame. Symbols show experimental data, curves are computed results.

2. Spatial variations of stable species in the rich ($\phi = 1.2$) propane flame. Symbols show experimental data, curves are computed results.

3. Spatial variations of temperature and major P-bearing species in the lean flame doped with 1200 ppm of TMP. Symbols show experimental data, curves are computed results.

4. Spatial variations of temperature and major P-bearing species in the rich flame doped with 1200 ppm of TMP. Symbols show experimental data, curves are computed results.

5. Experimentally determined, normalized burning velocity of laminar, stoichiometric propane/air flames due to addition of indicated additives.

6. Computed spatial profiles of major P-bearing species in the lean propane flame. Solid curves are results in TMP-doped flame, dashed curves for DMMP-doped flame.

7. Computed spatial profiles of major P-bearing species in the rich propane flame. Solid curves are results in TMP-doped flame, dashed curves for DMMP-doped flame.

TABLE 1.
Enthalpies of formation (H_f^o [kcal/mol])for phosphorus species, determined by various methods.

Species	BAC-MP4 [24]	CBS [38]	BAC-G2 (current work)	G3X2 [37]
PO	-3.02	-7.8	-8.83	-9.0
PO_2	-67.6	-70.3	-71.3	-69.6
PO_3	-102.8	-107.5	-107.5	
HOPO	-108.0	-112.4	-111.8	-112.3
$HOPO_2$	-165.0	-171.4	-171.9	-170.5
$PO[OH]_2$	-154.7		-157.9	-158.8
HPO	-18.0	-22.6	-23.0	
HPO_2	-97.1		-101.5	
P_2O_3	-147.2		-157.2	
P_2O_4	-204.3		-217.0	
P_2O_5	-256.2		-271.3	

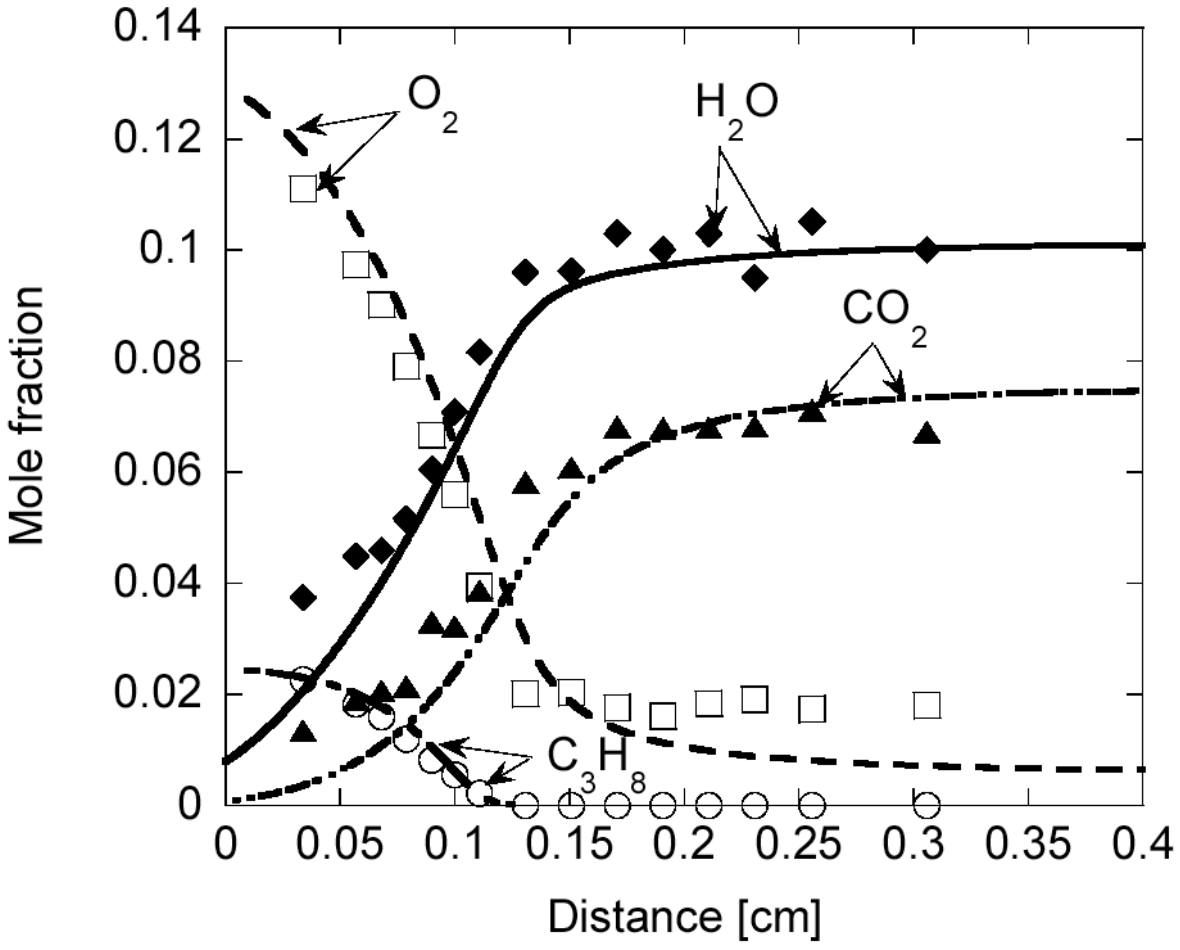
0.14
0.12
0.1
0.08
0.06
0.04
0.02
0
Mole fraction
0
0.05
0.1
0.15
0.2
0.25
0.3
0.35
0.4
Distance [cm]
O2
H2O
CO2
C3H8

Figure 1

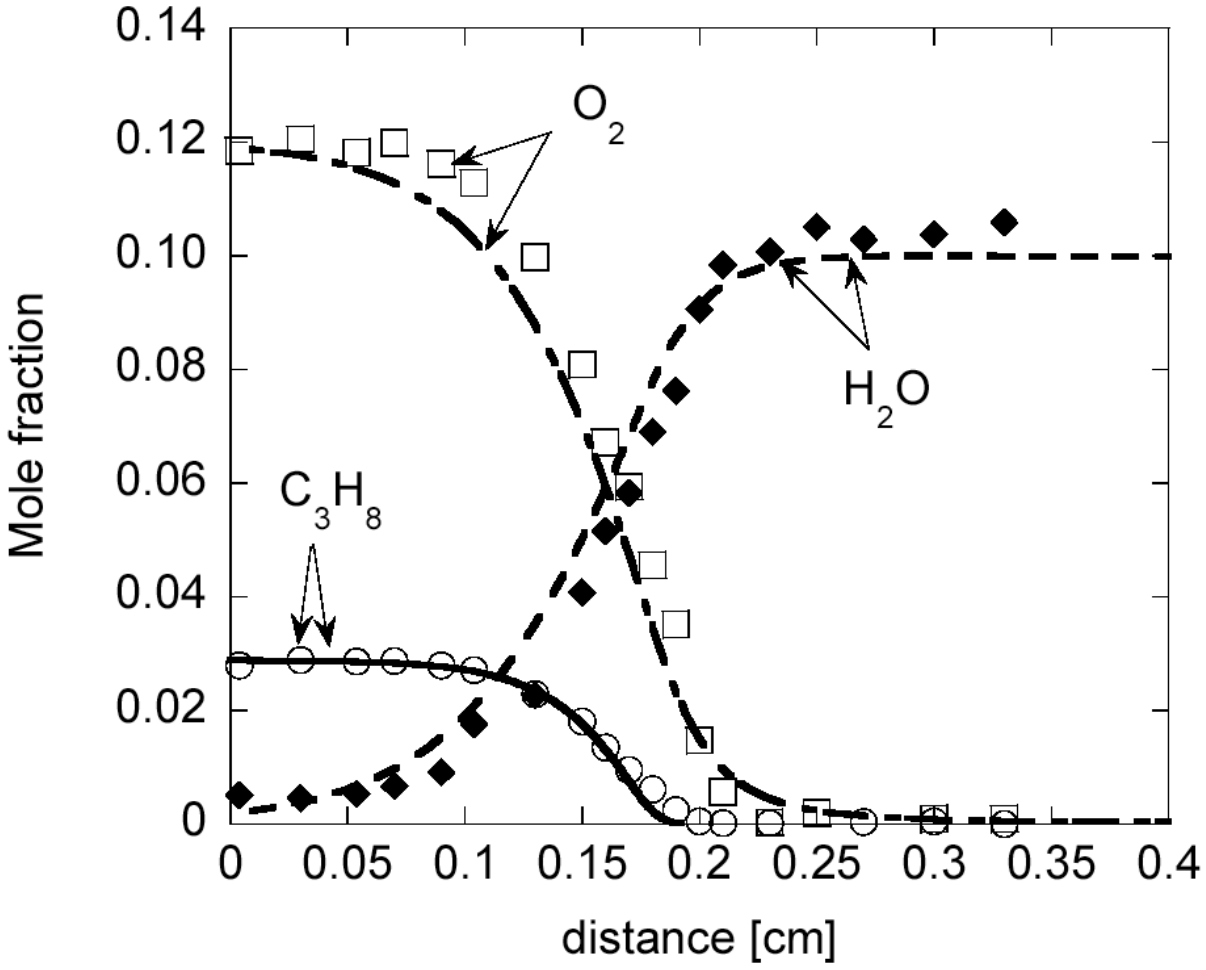
0.14
0.12
0.10
0.08
0.06
0.04
0.02
0
Mole fraction
O2
H2O
C3H8
0
0.05
0.1
0.15
0.2
0.25
0.3
0.35
0.4
distance [cm]

Figure 2

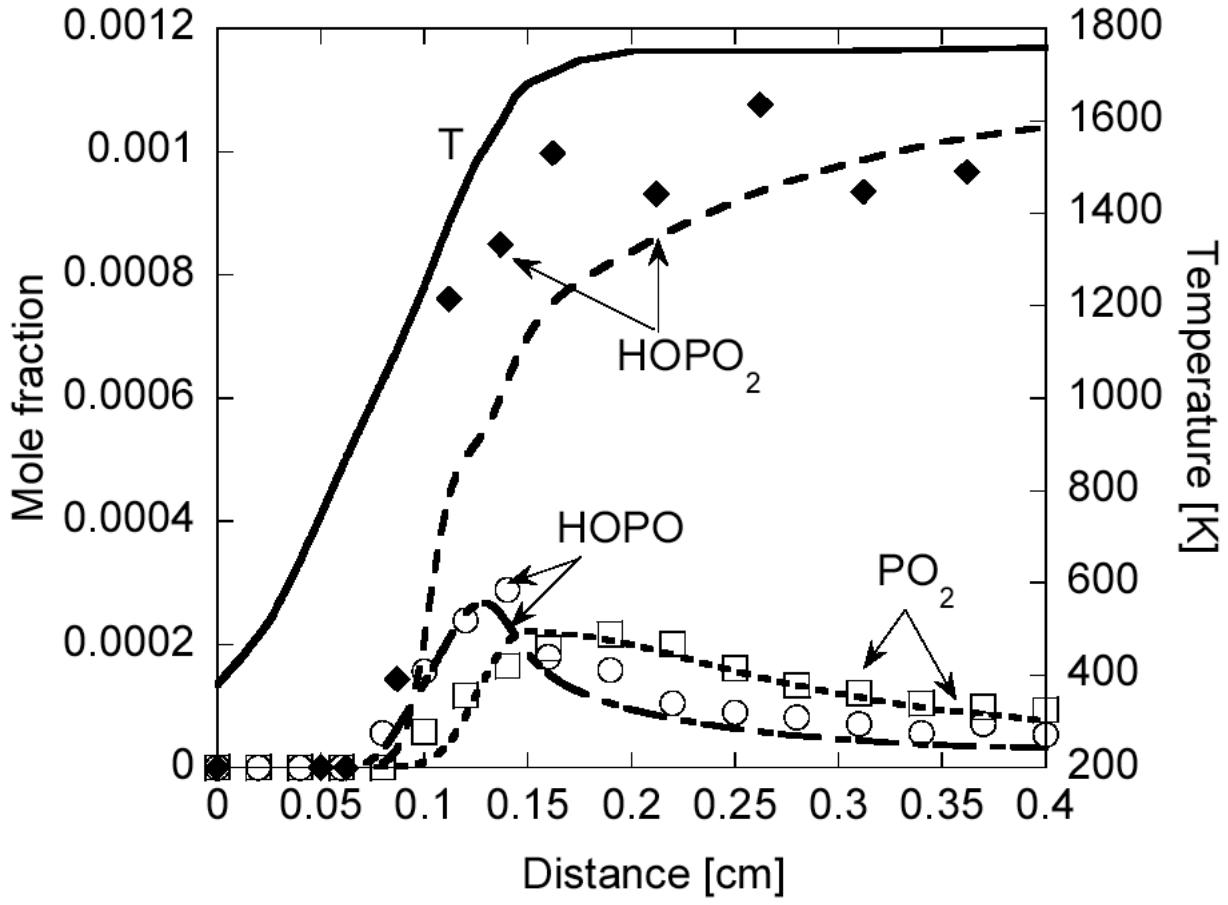
0.0012
0.001
0.0008
0.0006
0.0004
0.0002
0
Mole fraction
1800
1600
1400
1200
1000
800
600
400
200
Temperature [K]
0
0.05
0.1
0.15
0.2
0.25
0.3
0.35
0.4
Distance [cm]
T
HOPO2
HOPO
PO2

Figure 3

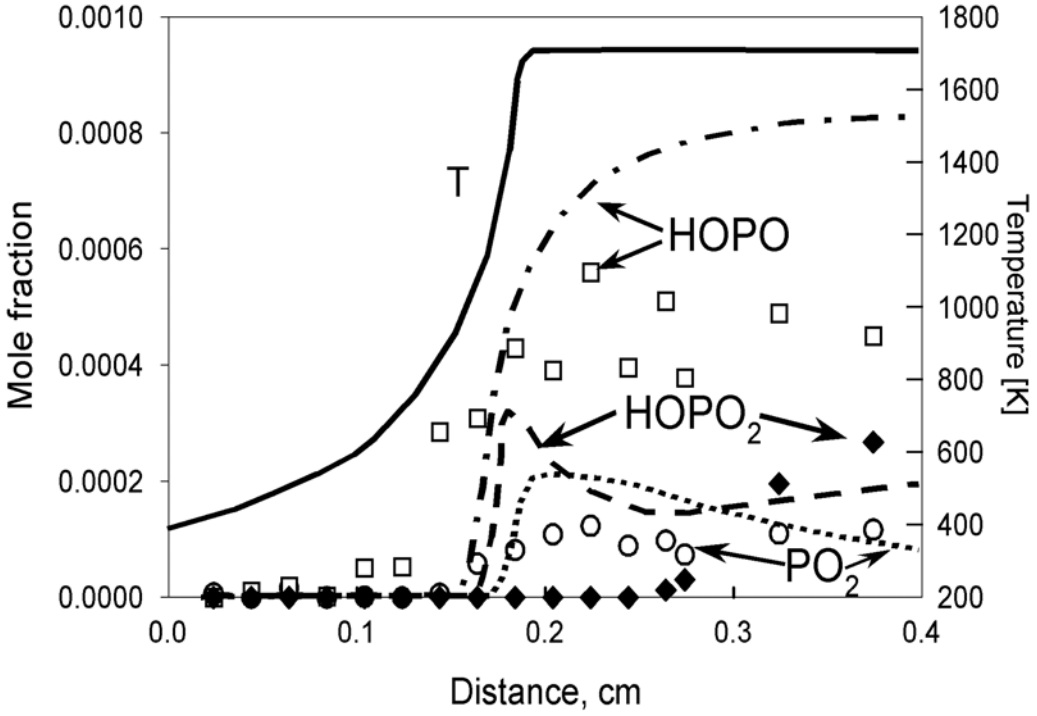
0.0010
0.0008
0.0006
0.0004
0.0002
0.0000
Mole fraction
0.0
0.1
0.2
0.3
0.4
Distance, cm
1800
1600
1400
1200
1000
800
600
400
200
Temperature [K]
T
HOPO
HOPO2
PO2

Figure 4

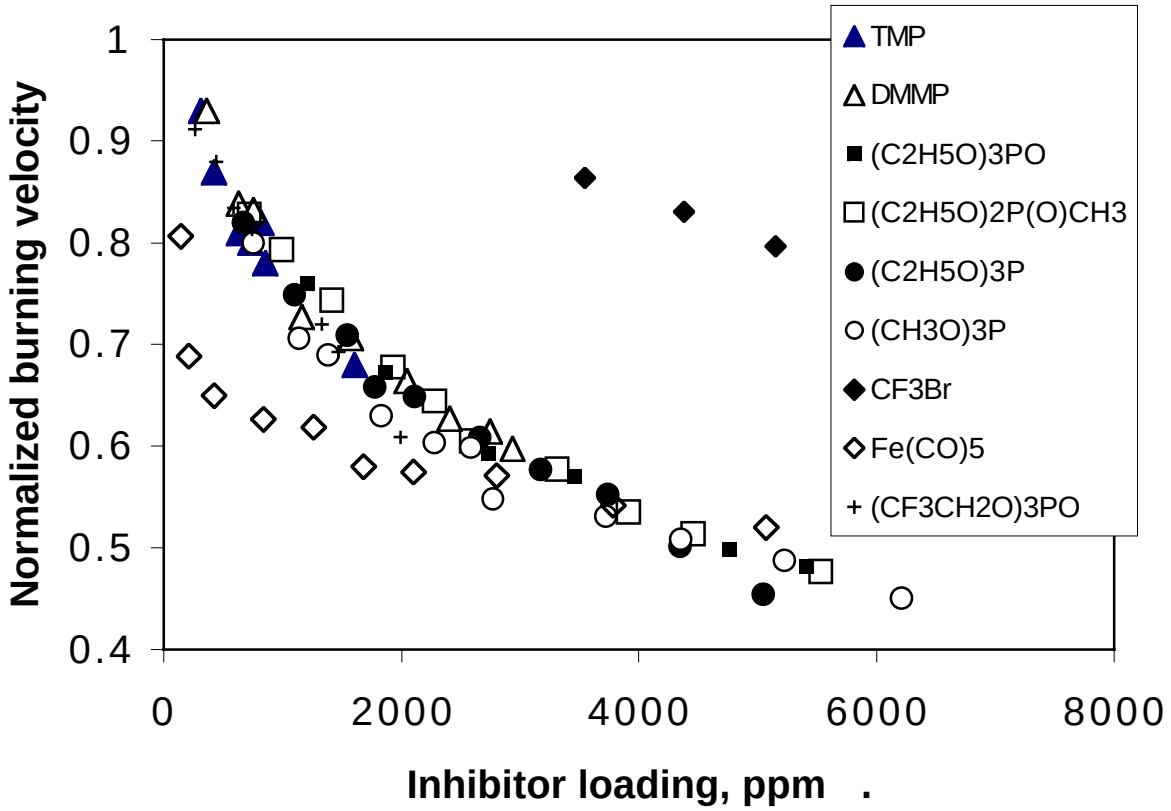
Normalized burning velocity
1
0.9
0.8
0.7
0.6
0.5
0.4
0
2000
4000
6000
8000
Inhibitor loading, ppm
TMP
DMMP
(C2H5O)3PO
(C2H5O)2P(O)CH3
(C2H5O)3P
(CH3O)3P
CF3Br
Fe(CO)5
+ (CF3CH2O)3PO

Figure 5

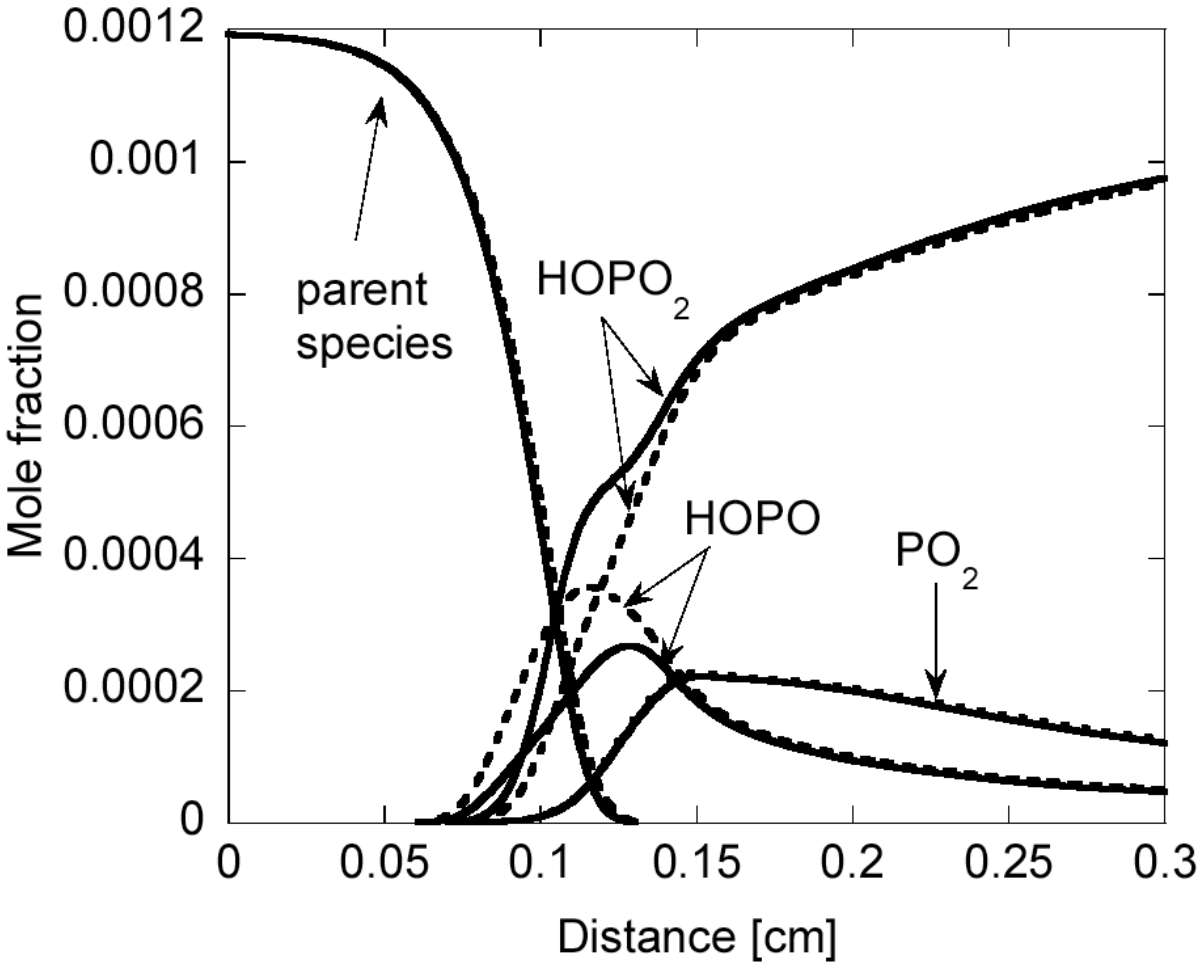
0.0012
0.001
0.0008
0.0006
0.0004
0.0002
0
Mole fraction
parent
species
HOPO2
HOPO
PO2
0
0.05
0.1
0.15
0.2
0.25
0.3
Distance [cm]

Figure 6

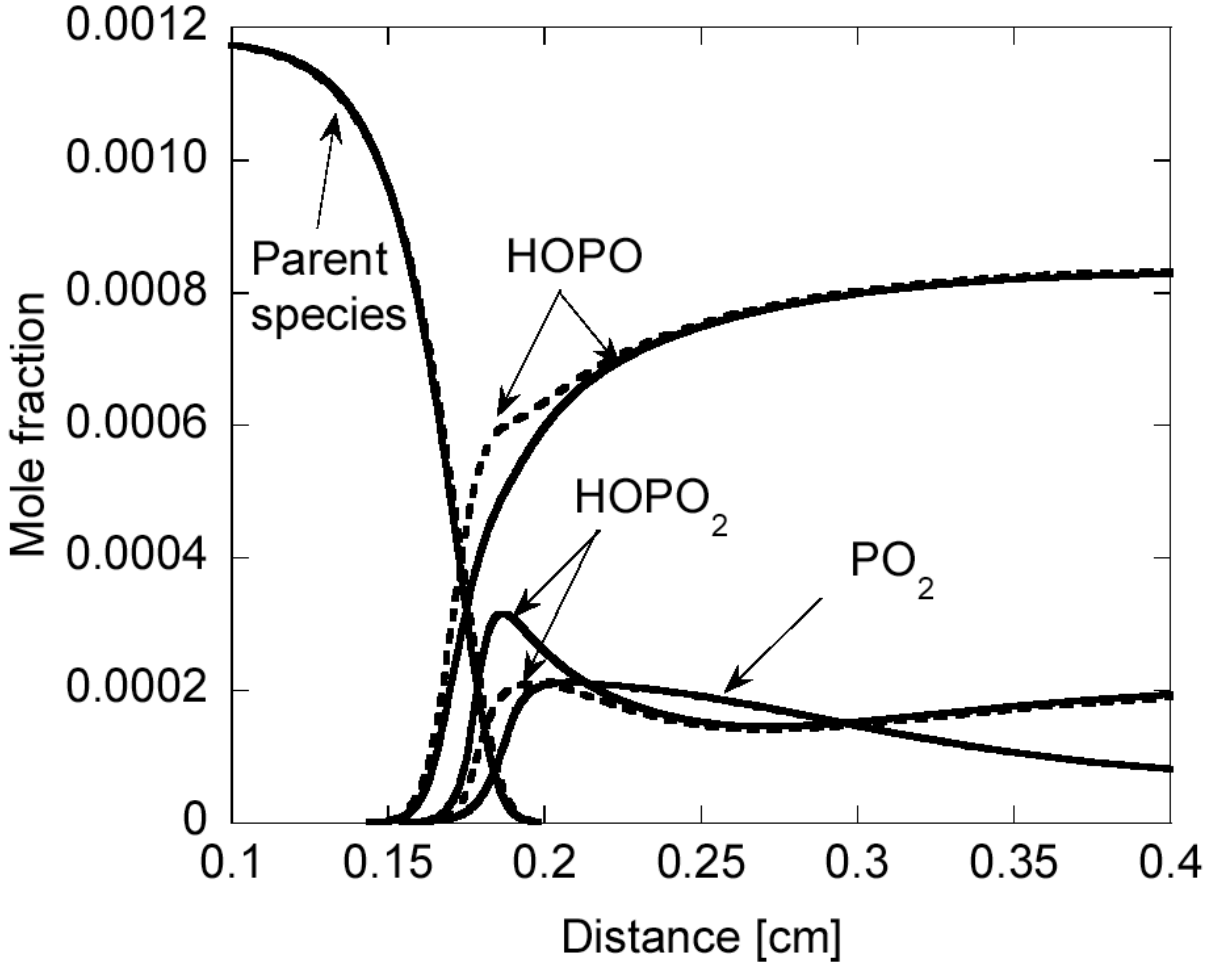
0.0012
0.0010
0.0008
0.0006
0.0004
0.0002
0
Mole fraction
Parent species
HOPO
HOPO2
PO2
0.1
0.15
0.2
0.25
0.3
0.35
0.4
Distance [cm]

Figure 7